Journal of Materials Chemistry C

Accepted Manuscript

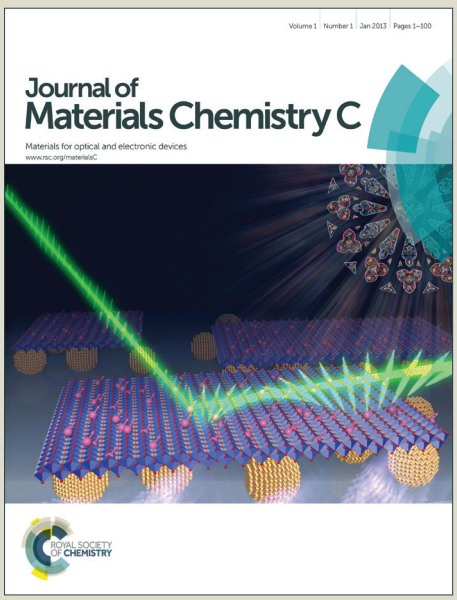

ROYAL SOCIETY OF CHEMISTRY

www.rsc.org/materialsC

Journal Name

RSCPublishing

COMMUNICATION

Ambipolar Organic Semiconductors with Cascade Energy Levels for Generating Long-Lived Charge Separated States: A Donor-Acceptor1-Acceptor2 Architectural Triarylamine Dye

Cite this: DOI: 10.1039/xoxxoooooox

Received ooth January 2012,
Accepted ooth January 2012

DOI: 10.1039/xoxxoooooox

www.rsc.org/

Tianyang Wang,[a] Krishanthi C. Weerasinghe,[b] Dongzhi Liu,[a] Wei Li,[a] Xilong Yan,[a] Xueqin Zhou*[a] and Lichang Wang*[b]

A donor-acceptor1-acceptor2 architectural 4-styryltriphenyl amine-based organic semiconductor was synthesized for solar cell applications. Sequential electron transfers together with effective hole transfer lead to a charge separated state lifetime of 650 ns, therefore boosting the short circuit current and efficiency of single layer organic photovoltaic cells.

Efficient conversion of sunlight requires an efficient photoinduced charge transfer and separation that are capable of generating long-lived charge separated states, therefore producing applicable photocurrents in solar cells or driving multi-electron chemistry of fuel synthesis.[1-6] Both electron donor and acceptor modules in a donor-acceptor (D-A) organic sensitizers determine the driving force of charge transfers,[4-11] while the distance, spatial orientation, and flexibility between the donor and acceptor significantly influence the efficiency and the rate of photoinduced charge transfers.[6-9] These parameters, governed by electronic coupling, reorganization energy, and attenuation factor, are key considerations in the optimization of efficient charge separation as well as in the elongation of lifetime of the corresponding radical ion pairs.[10-12] A key advancement in the field is the synthesis of organic sensitizer beyond utilizing π-conjugated linkers as they not only favor the throughbond electron migration from the donor to the acceptor, but also enhance back transfer, resulting in faster charge recombination.

Inspired by natural photosynthetic processes, where the formation of cascades of short-range photoinduced energy transfer and multistep electron transfer occurs, researchers have developed a large variety of supramolecular systems in the combination of various donors and acceptors.[4-23] Back electron transfer can be suppressed by cascade design of energy levels of sequential modules. Multi-donor designed systems (D1-D2-A) have been reported with cascade energy levels and therefore long-lived charge separated states, of which the electron migration rates among donors were too low to generate effective photocurrents in solar cells.[16-23] Although the efficiency of dye-sensitized solar cells has been exceeds 12% by multi-acceptor design with a D-A sensitizer and titanium oxide (TiO_2) as the second acceptor,[24] the limited electron transfer in the interface between the sensitizer and TiO_2 is still an issue and the short-lived charge separated states in such systems also present one of the major challenges in attaining highly efficient solar cells.

Herein, we report a metal-free and donor-acceptor1-acceptor2 (D-A1-A2) architectural organic semiconductor, 4,4'-dimethyl-4"-(4-(4-chloro-6-(2-(9,10-dioxoanthracen-1-ylamino)ethylamino)-1,3,5-triazin-2-ylamino)styryl)triphenylamine (MTPA-TRC-AEAQ), of which long-lived charge separated states were generated due to cascade electronic energy states and appropriate electron transfer rates inspire potential applications in photovoltaic cells. Design scheme of MTPA-TRC-AEAQ is shown in scheme 1.

Scheme 1 Design of MTPA-TRC-AEAQ with a cascade of electron transfers.

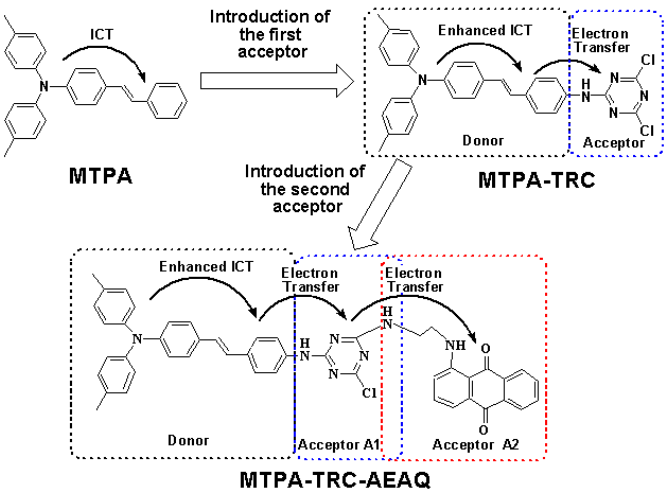

Donor module MTPA has been previously found with excellent electron-donating and hole-migrating abilities and its HOMO-LUMO transition involves intramolecular charge transfer (ICT) from the triphenylamine to the phenylene moiety.[25] Triazine (TRC) is a typical electron-accepting module and would be able to improve the electron-injection and electron-transportation abilities of its conjugated derivatives.[26,27] As such, it was chosen as the first acceptor. Anthraquinone derivative (AEAQ) is another common acceptor and has been reported with a lower LUMO than triaryl

modules.[18,19,25] Therefore, it was employed as the second acceptor. Our computational results of MTPA, TRC, AEAQ together with bonded molecules AEAQt, MTPA-TRC and MTPA-TRC-AEAQ (the optimized structures and calculated orbital contours can be found in the ESI, Fig. S1-S4) further confirmed the cascades of electronic energy levels, thus indicated that the designed organic molecule can thermodynamically facilitate electron transfers.

Upon synthesis of MTPA-TRC-AEAQ (the synthesis details can be found in the ESI), we first examined photophysical properties of this D-A1-A2 molecule together with four other species, MTPA, AEAQ, AEAQt, and the simple D-A molecule MTPA-TRC, using the absorption and fluorescence measurements. As shown in Fig. 1a, when the triazine module was bonded to MTPA, the absorption maximum of MTPA-TRC became 387 nm, which was red-shifted from 376 nm of MTPA. This is an indication of an enhanced ICT character, which was confirmed by the electron density reduction for the overlapping region of HOMO and LUMO. When a second acceptor AEAQ was attached to MTPA-TRC to form MTPA-TRC-AEAQ, the absorption maximum of this new compound is at 386 nm, which is very close to that of MTPA-TRC, illustrating insignificant perturbation to the D-A1 module. The characteristic band of MTPA-TRC-AEAQ at 500 nm is in between AEAQ (503 nm) and AEAQt (497 nm), an indication of the electronic and steric effects between the MTPA-TRC and AEAQ modules. However, these effects do not change the nature of various transitions as evidenced by similar shapes of the corresponding peaks.

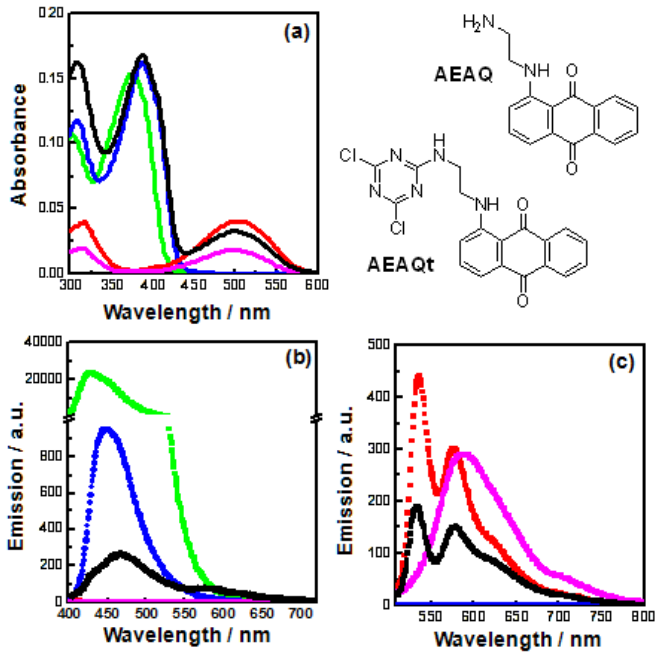

Fig. 1 Absorption (a) and fluorescence emission spectra excited at 380 nm (b) and 490 nm (c) of MTPA-TRC-AEAQ (black), MTPA-TRC (blue), MTPA (green), AEAQ (red) and AEAQt (magenta) in toluene (5×10^{-6} mol•L^{-1}).

As shown in Fig. 1b, the fluorescence maximum from the MTPA module of MTPA-TRC-AEAQ is at 464 nm, similar to that of MTPA-TRC, but is red-shifted from that of compound MTPA. The fluorescence intensity of MTPA is substantially quenched in MTPA-TRC and further quenched (~98%) in MTPA-TRC-AEAQ upon the excitation at 380 nm. Upon excitation at 490 nm, the fluorescence emission from the AEAQ module in MTPA-TRC-AEAQ shown in Fig. 1c splits into three peaks (535, 579, and 610 nm) with the maximum at 535 nm, which is consistent with the fluorescence characteristics of AEAQ, but is quenched by about 46%.

To understand the quenching mechanism, we carried out the time-resolved fluorescence experiments. The emission life times from these experiments are provided in Table 1. While a single exponential decay was observed for the MTPA compound, two-exponential decays were found for both MTPA-TRC and MPTA-TRC-AEAQ.

Table 1 The emission lifetimes of MTPA, MTPA-TRC, AEAQt and MTPA-TRC-AEAQ in toluene by fitting transient fluorescence spectra in Fig. S5 with exponential decay equations

Compounds	Emission lifetime, τ/ns		
	λ_{ex}=366 nm λ_{em}=460 nm	λ_{ex}=366 nm λ_{em}=700 nm	λ_{ex}=457 nm λ_{em}=700 nm
MTPA	1.80	—	—
MTPA-TRC	1.73, 0.29	—	—
AEAQt	—	—	4.90, 0.47
MTPA-TRC-AEAQ	1.61, 0.70	4.85, 0.30	4.84, 0.31

The two-exponential decays of the fluorescence spectra were often explained by an electron transfer from LUMO+1 to LUMO for various D-A dyes.[4,5] We expect electron transfer is also responsible for the fluorescence quench for MTPA-TRC based on our computational studies, which have been verified by electrochemical determination (see Fig.S6). As illustrated in Fig. 2, determined HOMO at MTPA and LUMO at TRC confirm a typical D-A chromophoric structure for MTPA-TRC. Accordingly, the fast decay component (0.29 ns) of the fluorescence from MTPA-TRC was assigned to the electron transfer from MTPA to TRC module, whereas the slow process (1.73 ns) was attributed to the salvation relaxation of the excited states.

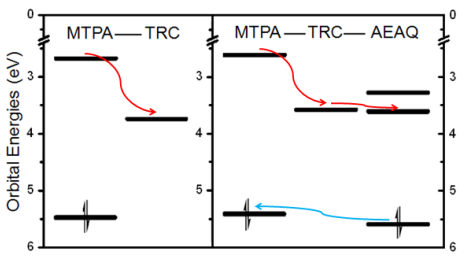

Fig. 2 Illustration of orbital energy levels of MTPA-TRC and MTPA-TRC-AEAQ determined electrochemically. The red and blue lines indicate the observed electron and hole transfers, respectively.

The results from the time resolved emission spectra of MTPA-TRC-AEAQ at 460 nm in Table 1 reveal that the fluorescence from MTPA module also decays biexponentially with lifetimes of 1.61 and 0.70 ns, respectively. For MTPA-TRC-AEAQ, the orbital level of TRC module could not be evaluated directly from the electrochemical determination of MTPA-TRC-AEAQ (Fig. S7). Then the TRC orbital level in MTPA-TRC-EA was employed given the effect to the substitution of the second chlorine at TRC by an ethylamine group. As shown in Fig. 2, MTPA-TRC-AEAQ has been confirmed experimentally with a typical D-A1-A2 chromophoric structure and MTPA, TRC and AEAQ modules play the roles of D, A1 and A2 respectively. Therefore the fast decay component is due to the electron transfer from MTPA to TRC followed by consecutive electron transfer to the AEAQ module. The longer lifetime of the fast component in MTPA-TRC-AEAQ than that in MTPA-TRC is due to a slightly higher TRC LUMO in MTPA-TRC-AEAQ with respect to MTPA-TRC, shown in Fig.2, which reduces the driving force for the electron to transfer from MTPA LUMO and thus slows

the process. The lifetime of the slow component, which is attributed to the salvation relaxation of the MTPA singlet, is slightly shorter than that for MTPA-TRC. This is due to the intramolecular photoinduced Forster energy transfer from excited MTPA to the AEAQ module, which was further confirmed by the appearance of a weak characteristic peak from the AEAQ module that emerged concurrently at about 579 nm in the MTPA-TRC-AEAQ spectrum (Fig. 1b), whereas little absorption and fluorescence were detected for either AEAQt or AEAQ. Similar biexponential decay kinetics of the fluorescence was also found at 700 nm from the AEAQ module; the lifetime of fast components (0.31 ns) is shorter than the corresponding value of AEAQt (0.47 ns). Additionally, the lower HOMO of the AEAQ module than that of the MTPA module allows hole transfer from the excited AEAQ to MTPA, making MTPA-TRC-AEAQ ambipolar.

To determine the lifetime of charge separated state in compounds MTPA-TRC and MTPA-TRC-AEAQ, we performed nanosecond transient absorption measurements. Fig. 3a depicts the characteristics of $MTPA^{\cdot+}$ absorption in MTPA-TRC compound in the range 440-700 nm with the negative ΔOD corresponding to the bleach of ground states. Fig. 3b shows the formation of charge-separated states $MTPA^{\cdot+}$-$TRC^{\cdot-}$ with an estimated lifetime of 80 ns.

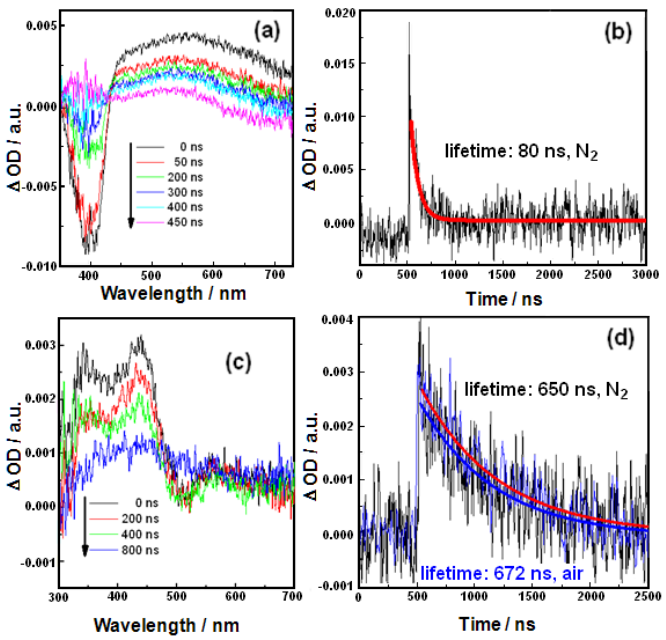

Fig. 3 Nanosecond transient absorption spectra (a) and kinetics at 600 nm (b) of MTPA-TRC (1×10^{-5} mol•L^{-1}) and the nanosecond transient absorption spectra (c) and kinetics at 440 nm (d) of MTPA-TRC-AEAQ (1×10^{-5} mol•L^{-1}) in nitrogen following excitation with 410 nm, 8 ns laser pulses. The solid lines are the fitting curves by single-order exponential decay equation and the blue line in (d) was obtained in air. The solvent is toluene.

When the second acceptor, AEAQ, was attached to MTPA-TRC, a significantly different transient absorption spectra and kinetics were observed. The significant different features in Fig. 3c with respect to Fig. 3a are due to the addition of $AEAQ^{\cdot-}$ absorption at 340 nm and 440 nm and the bleach of AEAQ ground state at 500 nm, which were also observed previously for the AEAQ system.[28,29] The slightly weaker $MTPA^{+}$ signal in MTPA-TRC-AEAQ is due to the overlap of the $MTPA^{+}$ absorption with the bleach of AEAQ ground state. Furthermore, it could also indicate that the decay ratio between electron transfer and salvation relaxation is decreased slightly in MTPA-TRC-AEAQ. Similar spectra obtained in the presence of oxygen confirm the formation of the charge separated states $MTPA^{\cdot+}$-TRC-$AEAQ^{\cdot-}$, of which the lifetime was evaluated to be 650 ns. The transient absorption difference spectra excited at 500 nm (Fig. S8) also exhibit the absorption features of $AEAQ^{\cdot-}$ and $MTPA^{\cdot+}$ above 420 nm. All these illustrated a hole transfer from the excited AEAQ to the MTPA module. The lifetime of the resulted charge separated states $MTPA^{\cdot+}$-TRC-$AEAQ^{\cdot-}$ due to hole transfer was found to be around 680 ns.

The eightfold elongation of lifetime in MTPA-TRC-AEAQ over MTPA-TRC is determined in toluene. These lifetimes change with solvent and will differ in solid state. We expect some changes in the lifetimes for both materials when they are assembled to solar cell devices, but still expect a significantly longer charge separation in MTPA-TRC-AEAQ. To illustrate the promise of the MTPA-TRC-AEAQ due to its superior charge separation property, we assembled single layer organic photovoltaic cells (SLOPV) using both materials and conducted preliminary tests on these devices. As shown in Fig. 4, the dye was placed between ITO and Ag electrodes with a thickness of about 250 nm by spin coating it from tetrahydrofuran. The photovoltaic characteristics under AM 1.5 G illumination (100 mW/cm^2) are given in Table 2 (the J-V curves of SLOPV can be found in Fig. S9). The maximum incident photon-to-electron conversion efficiency was found as 46% at 410 nm for MTPA-TRC-AEAQ devices (Fig. 4) and the photovoltaic characteristics of MTPA-TRC-AEAQ are higher in SLOPV than reported data of compounds showing long-lived charge-separated states.[30-32] MTPA-TRC SLOPV was also fabricated as a comparison. As shown in Table 2, the short circuit current J_{cc} and power conversion efficiency η were far lower with MTPA-TRC than MTPA-TRC-AEAQ. MTPA-TRC exhibits similar photovoltaic characteristics in Schottky organic solar cells with common organic semiconductors such as phthalocyane, poly(phenylene vinylene) and triarylamine derivatives,[33-36] of which the efficiency has been improved to 6% above and even exceeds 10% by combined application of other semiconductors and proper design of solar cell structures.[36-40] The far better photovoltaic characteristics of MTPA-TRC-AEAQ than MTPA-TRC suggests potential applications in solar cells.

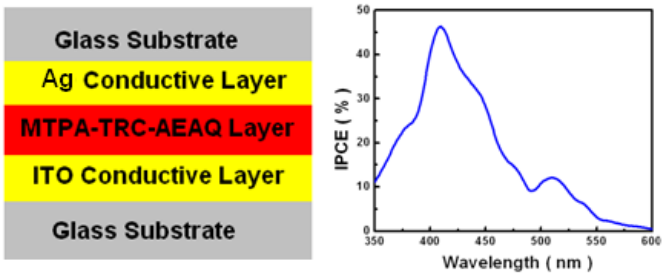

Fig. 4 Device structure and IPCE curve of obtained single layer organic photovoltaic cells.

Table 2 Photovoltaic performances of single layer organic photovoltaic cells ITO/Semiconductor/Ag under AM 1.5 G illumination

Semiconductors	V_{oc} /V	J_{cc}/mA/cm^2	FF /%	η/%
MTPA-TRC-AEAQ	0.90	1.88	52.40	0.89
MTPA-TRC	0.80	0.068	46.66	0.03

Conclusions

In conclusion, we designed, synthesized, and characterized the D-A1-A2 architectural MTPA-TRC-AEAQ. Cascaded electronic energy levels lead to sequential electron transfers starting from

^{1}MTPA* to TRC and then to AEAQ module as well as hole transfer from ^{1}AEAQ* to MTPA module. The lifetime of charge separated states of this newly designed ambipolar MTPA-TRC-AEAQ is elongated to 650 ns, an eightfold of that of the donor-acceptor MTPA-TRC parent molecule (80 ns). The photovoltaic tests indicate potential applications of MTPA-TRC-AEAQ in solar cells. Our approach to design D-A1-A2 architectural organic semicondutors offers a simple yet effective platform to develop novel multichromophore materials for organic solar cells and other optoelectronic devices.

Acknowledgements

This work was supported by National Nature Sciences Foundation of China (N0. 20976122) and the Science and Technology Department of Tianjin University for travel (L.W.)

Notes and references

[a] School of Chemical Engineering and Technology, Tianjin University, Tianjin 300072, China. E-mail: zhouxueqin@tju.edu.cn

[b] Department of Chemistry and Biochemistry, Southern Illinois University, 1245 Lincoln Drive, Carbondale, IL 62901, United States. E-mail: lwang@chem.siu.edu

Electronic Supplementary Information (ESI) available: [Experimental and computational details with complete spectroscopic and structural analysis]. See DOI: 10.1039/c000000x/

1 C.A. Rozzi, S.M. Falke, N. Spallanzani, A. Rubio, E. Molinari, D. Brida, M. Maiuri, G. Cerullo, H. Schramm, J. Christoffers and C. Lienau, *Nat. Commun.*, 2013, **4**, 1602.

2 J. Huang, K.L. Mulfort, P. Du and L.X. Chen, *J. Am. Chem. Soc.*, 2012, **134**, 16472.

3 K. Cnops, B.P. Rand, B. Cheyns, D. Verreet, M.A. Empl and P. Heremans, *Nat. Commun.*, 2014, **5**, 3406.

4 L. Yu, J. Xi, H.T. Chan, T. Su, L.J. Antrobus, B. Tong, Y. Dong, W.K.Chan, and D.L. Phillips, *J. Phys. Chem. C*, 2013, **117**, 2041.

5 V. Hrobáriková, P. Hrobárik, P. Gajdoš, L. Fitilis, M. Fakis, P. Persephonis and P. Zahradnik, *J. Org. Chem.*, 2010, **75**, 3053.

6 H. Tamura and I. Burghardt, *J. Am. Chem. Soc.*, 2013, **135**, 16364.

7 A. Jailaubekov, A.P. Williard, J. Tritsch, W.L. Chan, N. Sai, L. Kaake, R.I. Gearba, K. Leung, P.J. Rossky and X.Y. Zhu, *Nat. Mater.*, 2013, **12**, 66.

8 M. Emanuele, N. Martsinovich and A. Troisi, *Angew. Chem. Int. Ed.*, 2013, **52**, 973.

9 M. Kimura, H. Namoto, N. Masaki and S. Mori, *Angew. Chem. Int. Ed.*, 2012, **51**, 4371.

10 A.O. Kichigina, V.N. Ionkin and A.I. Ivanov, *J. Phys. Chem. B*, 2013, **117**, 7426.

11 S. Fukuzumi, *Phys. Chem. Chem. Phys.*, 2008, **10**, 2283.

12 S. Castellanos, A.A. Vieira, B.M. Illescas, V. Sacchetti, C. Schubert, J. Moreno, D.M. Guldi, S. Hecht and N. Martin, *Angew. Chem. Int. Ed.*, 2013, 52, 13985.

13 Y. Tao, J. Xiao, C. Zheng, Z. Zhang, M.K. Yan, R.F. Chen, X.H. Zhou, H.H. Li, Z.F. An and Z.X. Wang, *Angew. Chem. Int. Ed.*, 2013, **52**, 10491.

14 M. Rudolf, L. Feng, Z. Slanina, T. Akasaka, S. Nagase and D.M. Guldi, *J. Am. Chem. Soc.*, 2013, **135**, 11165.

15 A. Mishra and P. Bauerle, *Angew. Chem. Int. Ed.*, 2012, **51**, 2020.

16 P.K. Poddutoori, N. Zarrabi, A.G. Moiseev, R. Gumbau-Brisa, A. Vassiliev and S. van der Est, *Chem. Eur. J.*, 2013, **19**, 3148.

17 M.B. Majewski, N.R. de Tacconi, F.M. MacDonnell and M.O.Wolf, *Chem. Eur. J.*, 2013, **19**, 8331.

18 J. Hankache, M. Niemi, H. Lemmetyinen and O.S.S.Wenger, *Inorg. Chem.*, 2012, **51**, 6333.

19 J. Hankache and O.S. Wenger, *Chem. Commun.*, 2011, **47**, 10145.

20 M. Borgstrom, N. Shaikh, O. Johansson, M.F. Anderlund, S. Styring, B. Akermark, A. Magnuson and L. Hammarstrom, *J. Am. Chem. Soc.*, 2005, **127**, 17504.

21 H. Imahori, D.M. Guldi, K. Tamaki, Y. Yoshida, C. Luo, Y. Sakata and S. Fukuzumi, *J. Am. Chem. Soc.*, 2001, **123**, 6617.

22 J. Hankache, M. Niemi, H. Lemmetyinen and O.S.S. Wenger, *J. Phys. Chem. A*, 2012, **116**, 8159.

23 M.E. El-Khouly, D.K. Ju, K.Y. Kay, F. D'Souza and S. Fukuzumi, *Chem. Eur. J.*, 2010, **16**, 6193.

24 A. Yella, H. Lee, H.N. Tsao, C. Yi, A.K. Chandiran, M. Nazeeruddin, E.W. Diau, C. Yeh, S.M. Zakeeruddin and M. Grätzel, *Science*, 2011, **334**, 629.

25 L.L. Walkup, K.C. Weerasinghe, M. Tao, X. Zhou, M. Zhang, D. Liu and L. Wang, *J. Phys. Chem. C*, 2010, **114**, 19521.

26 H.P. Zhou, Z. Zheng, G. Xu, Z. Yu, X. Yang, L. Cheng, X. Tian, L. Kong, J. Wu and Y. Tian. *Dyes Pigm.*, 2012, **94**, 570.

27 T. Lazarides, G. Charalambidis, A. Vuillamy, M. Réglier, F. Klontzas, G. Froudakis, S. Kuhri, D.M. Guldi and A.G. Coutsoleos, *Inorg. Chem.*, 2011, **50**, 8926.

28 T. Nakayama, K. Ushida, K. Hamanoue, M. Washio, S. Tagawa and Y. Tabata, *J. Chem. Soc. Faraday Trans.*, 1990, **86**, 95.

29 A. Chowdhury and S. Basu, *J. Lumines.*, 2006, **121**, 113.

30 A.M. Ramos, M.T. Rispens, J.K.J. van Duren, J.C. Hummelen and R.A.J. Janssen, *J. Am. Chem. Soc.*, 2001, **123**, 6714.

31 S. Roquet, A. Cravino, P. Leriche, O. Aleveque, P. Frere and J. Roncali, *J. Am. Chem. Soc.*, 2006, **128**, 3459.

32 C. He, Q. He, X. Yang, G. Wu, C. Yang, F. Bai, Z. Shuai, L. Wang and Y. Li, *J. Phys. Chem. C.*, 2007, **111**, 8661.

33 S. Antohe, *J. Optoelectron. Adv. Mater.*, 2000, **2**, 498.

34 S. Karg, W. Riess, V. Dyakonov and M. Schwoerer, *Synthe. Met.*, 1993, **54**, 427.

35 A.K. Ghosh, D.L. Morel, T. Feng, R.F. Shaw and C.A. Rowe, *J. Appl. Phys.*, 1974, **45**, 230.

36 A. Mishra and P. Bauerle, *Angew. Chem. Int. Ed.*, 2012, **51**, 2020.

37 A. Saeki, M. Tsuji, S. Yoshikawa, A. Gopal and S. Seki, *J. Mater. Chem. A*, 2014, **2**, 6075.

38 K. Cnops, B.P. Rand, D. Cheyns, B. Verreet, M.A. Empl and P. Heremans, *Nat. Commun.*, 2014, **5**, 3406.

39 H. Zhou, L. Yang, A.C. Stuart，S.C. Price, S. Liu and W. You, *Angew. Chem. Int. Ed.*, 2011, **50**, 2995.

40 J. You, L. Dou, K. Yoshimura, T. Kato, K. Ohya, T. Moriarty, K. Emery, C.C. Chen, J. Gao, G. Li and Y. Yang, *Nat. Commun.*, 2013, **4**, 1446.

Journal Name

RSCPublishing

COMMUNICATION

An ambipolar semiconductor with cascade electronic energy levels generates long-lived charge separated state for solar cell applications.